Neuron, Vol. 42, 913–926, June 24, 2004, Copyright ©2004 by Cell Press

The Microtubule Plus End Tracking Protein Orbit/MAST/CLASP Acts Downstream of the Tyrosine Kinase Abl in Mediating Axon Guidance

Haeryun Lee,[1] Ulrike Engel,[1] Jannette Rusch, Simone Scherrer, Katherine Sheard, and David Van Vactor*
Department of Cell Biology
Program in Neuroscience
Dana Farber Cancer Institute/Harvard Cancer Center and Harvard Center of Neurodegeneration and Repair
Harvard Medical School
240 Longwood Avenue
Boston, Massachusetts 02115

Summary

Axon guidance requires coordinated remodeling of actin and microtubule polymers. Using a genetic screen, we identified the microtubule-associated protein Orbit/MAST as a partner of the Abelson (Abl) tyrosine kinase. We find identical axon guidance phenotypes in *orbit/MAST* and *Abl* mutants at the midline, where the repellent Slit restricts axon crossing. Genetic interaction and epistasis assays indicate that Orbit/MAST mediates the action of Slit and its receptors, acting downstream of Abl. We find that Orbit/MAST protein localizes to *Drosophila* growth cones. Higher-resolution imaging of the Orbit/MAST ortholog CLASP in *Xenopus* growth cones suggests that this family of microtubule plus end tracking proteins identifies a subset of microtubules that probe the actin-rich peripheral growth cone domain, where guidance signals exert their initial influence on cytoskeletal organization. These and other data suggest a model where Abl acts as a central signaling node to coordinate actin and microtubule dynamics downstream of guidance receptors.

Introduction

In order to establish an intricate yet specific network of neuronal connections, axons are guided from intermediate to final targets by an assortment of attractive and repellent factors (reviewed by Dickson, 2002). The navigational response to such guidance cues depends on a complex and dynamic cytoskeletal machine within the growth cone that is linked via signaling pathways to receptors at the cell surface. In essence, the growth cone acts as an exquisitely sensitive molecular compass, translating the spatial asymmetry of extracellular cues into polarization of the cytoskeletal elements that determine the directional specificity of cell movement. Two major targets in this cell polarity machine are the microfilament networks that support the growth cone perimeter and the microtubule arrays that build the core of the nascent axon (reviewed by Suter and Forscher, 2000). While a comprehensive understanding of cytoskeletal signaling is still elusive, much progress has been made in identifying pathways and effector molecules that control the rapid and initial response of actin assembly to particular guidance factors (reviewed by Dickson, 2002; Patel and Van Vactor, 2002). However, very little progress has been made in identifying microtubule-associated proteins (MAPs) that participate in specific pathways (see reviews by Dent and Gertler, 2003; Lee and Van Vactor, 2003).

The actin networks that propel membrane protrusion are thought to mount the initial response to guidance information (e.g., Fan et al., 1993; Fan and Raper, 1995; Lin and Forscher, 1993; O'Connor and Bentley, 1993). Actin remodeling in the growth cone peripheral (P) domain remains dynamic and unstable, allowing for rapid changes in direction or cell contact. Microtubules are also dynamic in the periphery, and their recruitment and subsequent bundling to establish the central (C) domain of the growth cone represent a hallmark of directional growth (Tanaka et al., 1995; Suter and Forscher, 1998). Consequently, as growth cones make guidance decisions in situ and select particular filopodia to define the new direction of movement, it is the consolidation of microtubule structures and concomitant dilation of filopodia that are most predictive of a change in direction (Sabry et al., 1991; Myers and Bastiani, 1993; Murray et al., 1998). Indeed, perturbation of microtubule dynamics has a dramatic effect on growth cone navigational behavior (Tanaka et al., 1995; Williamson et al., 1996; Dent and Kalil, 2001; Buck and Zheng, 2002).

In the transition zone between the P and C domains of the growth cone, a specialized class of microtubules extend and penetrate into the actin-rich perimeter. Recent studies in growth cones and nonneuronal cells show that such "pioneer" microtubules enjoy an intimate relationship with specialized actin structures that support individual filopodia and define the region between P and C domains (Dent and Kalil, 2001; Schaefer et al., 2002; Zhou et al., 2002), supporting theoretical models that predict crosstalk between the two polymer networks (Hely and Willshaw, 1998). Consistent with this idea, pharmacological studies show that growth cone microtubule structures and guidance are dependent on actin dynamics (Zhou et al., 2002). Interestingly, nonneuronal studies suggest that a reciprocal signaling relationship exists at this cytoskeletal interface and that molecules such as Rho family GTPases act to coordinate the dynamics of both actin and microtubules (e.g., Wittmann et al., 2003). Signaling molecules or "nodes" that coordinate multiple downstream events are common in signal transduction pathways (reviewed by Jordan et al., 2000). While Rho family GTPases are well known for this capacity (reviewed by Etienne-Manneville and Hall, 2002), additional classes of proteins are also likely to serve this function during axon guidance.

One excellent candidate as an axon guidance signaling node in *Drosophila* is the Abelson (Abl) protein tyrosine kinase (reviewed by Lanier and Gertler, 2000; Moresco and Koleske, 2003). Abl is required for the accurate guidance of both central and peripheral axon

*Correspondence: davie@hms.harvard.edu
[1]These authors contributed equally to this work.

pathways (Wills et al., 1999a, 2002; Hsouna et al., 2003) and modulates the function of several axonal receptors (Elkins et al., 1990; Giniger, 1998; Wills et al., 1999b, 2002; Bashaw et al., 2000; Crowner et al., 2003; Hsouna et al., 2003; Liebl et al., 2003). Study of these signaling pathways shows that Abl interacts genetically with a number of intracellular effector proteins, including Enabled, Profilin, Trio, and the cyclase-associated protein (Gertler et al., 1995; Wills et al., 1999a, 2002; Liebl et al., 2000).

So far, the majority of known Abl interactors control aspects of actin assembly. However, we have recently discovered a new Abl interactor known to associate with microtubules, suggesting a link that might coordinate actin and microtubule dynamics. Genetic analysis has identified a number of MAPs that are necessary for axonogenesis, including Futsch/MAP1b (Hummel et al., 2000), Short stop (Lee et al., 2000), and Pod-1 (Rothenberg et al., 2003). Although some of these effector proteins are targets for intracellular kinases (e.g., MAP1b; Goold and Gordon-Weeks, 2001), none have been shown to act downstream of specific axon guidance factors. While the Semaphorin effector Collapsin response mediator protein (CRMP; Goshima et al., 1995) has been shown to bind Tubulin heterodimers and influence polymer assembly (e.g., Fukata et al., 2002b), the primary role of the CRMP family is thought to involve membrane dynamics (e.g., Nishimura et al., 2003).

We previously described a kinase-dependent gain-of-function (GOF) phenotype for Abl in the *Drosophila* retina that displays sensitive genetic interactions with receptors in the Roundabout (Robo) family (Wills et al., 2002). Loss-of-function (LOF) studies confirm that Abl plays a complex role in axon guidance at the midline, where Robo receptors mediate the repellent action of Slit (Bashaw et al., 2000; Wills et al., 2002; Hsouna et al., 2003). Moreover, there is an endogenous role for *Abl* in the retina, suggesting that this neural tissue can be used as a tool to identify additional classes of effectors in the Abl pathway (Henkemeyer et al., 1987). Here, we describe one of the genes derived from an ongoing retinal screen for modifiers of Abl^{GOF}: the MAP *Orbit/MAST* (also known as *Chromosome Bows* [*Chb*]; Fedorova et al., 1997; Inoue et al., 2000; Lemos et al., 2000), ortholog of the vertebrate *cytoplasmic linker protein* (*CLIP*)*-associated proteins* (*CLASPs*; Akhmanova et al., 2001). Using zygotic null alleles to escape a requirement during oogenesis, we discover that Orbit/MAST is necessary for accurate axon guidance at the midline choice point. Phenotypic characterization, genetic interactions, and genetic epistasis experiments suggest that this MAP acts downstream of Abl in the Slit repellent pathway, consistent with its localization to axons and growth cones. Parallel imaging studies in *Xenopus* growth cones show that vertebrate CLASP identifies a subset of axonal microtubules that extend into the peripheral domain, where actin dynamics are known to influence microtubule behavior. Finally, we show that elevation of CLASP activity in *Xenopus* neurons reduces not only microtubule advance but also growth cone translocation.

Results

Orbit/MAST Is Required for Accurate Midline Axon Guidance

We identified Orbit/MAST as a candidate partner of Abl in a screen outside of the embryo where we had first defined a requirement for the kinase in axonogenesis (Wills et al., 1999a). In our retinal screen, overexpression of *orbit/MAST* enhanced the Abl^{GOF} phenotype, suggesting that these two proteins cooperate in vivo (J.R., K.S., H.L., and D.V.V., unpublished data). However, validation of the screen required analysis of mutations in *orbit/MAST*.

Orbit/MAST was initially identified as a maternal-effect lethal locus with defects in mitotic spindle and chromosome morphology (Fedorova et al., 1997; Inoue et al., 2000; Lemos et al., 2000); however, zygotic mutants display no defects in cell division, presumably due to maternal stores of the protein required for oogenesis (Maiato et al., 2002). We therefore examined independent LOF alleles for zygotic phenotypes. Axon fascicles that are restricted to either side of the central nervous system (CNS) midline by Slit signaling can be visualized at stage 17 with anti-Fasciclin II (FasII, Mab1D4). In late-stage wild-type embryos (stage 17), FasII is excluded from the midline (Figure 1A). However, in *orbit/MAST* mutants, we discovered ectopic midline crossing, primarily by the midline-proximal MP1 axon pathway (Figures 1B and 1C). This phenotype is qualitatively identical to that seen in *Abl* zygotic mutants (Figure 1D; Wills et al., 2002; Hsouna et al., 2003; note that loss of maternal and zygotic Abl generates catastrophic axonal defects, underlining Abl's central role in axonal development; Grevengoed et al., 2001). Since the exclusion of FasII from axon commissures reflects a redistribution of protein that could be dependent on Orbit/MAST, it was important to confirm the guidance defects with an alternative marker. Using a Tau-LacZ fusion protein under control of an Apterous promotor expressed in two medial ipsilateral axons that never cross the midline (Figure 1E; Lundgren et al., 1995), we found frequent ectopic crossing of these axons in *orbit/MAST* mutants (Figure 1F).

In order to rule out the possibility that axonal defects in *orbit/MAST* alleles result from some early failure in cell division or fate acquisition in the CNS, we stained these homozygous mutants with markers of neuronal cell fate. The number and position of neurons appeared to be normal even in the strongest *orbit/MAST* alleles (e.g., Figures 1G and 1H). We also checked the fate of the midline glia that secrete Slit, but no abnormalities were detected (see below). To prove that the *orbit/MAST* axon defects represent a late, CNS-specific function of the gene, we expressed UAS-*orbit(+)* in mutant backgrounds under the control of postmitotic, neuron-specific GAL4 (elav-GAL4 and 1407-GAL4; Luo et al., 1994). Quantification of ectopic midline crossing in independent *orbit/MAST* mutants revealed an allelic series of guidance defects whose penetrance was consistent with the perdurance of some maternal protein (Figure 1I). However, two independent transgenes successfully rescued the axon guidance defects of null *orbit/MAST* alleles (Figure 1I, asterisks). Thus, Orbit/MAST is re-

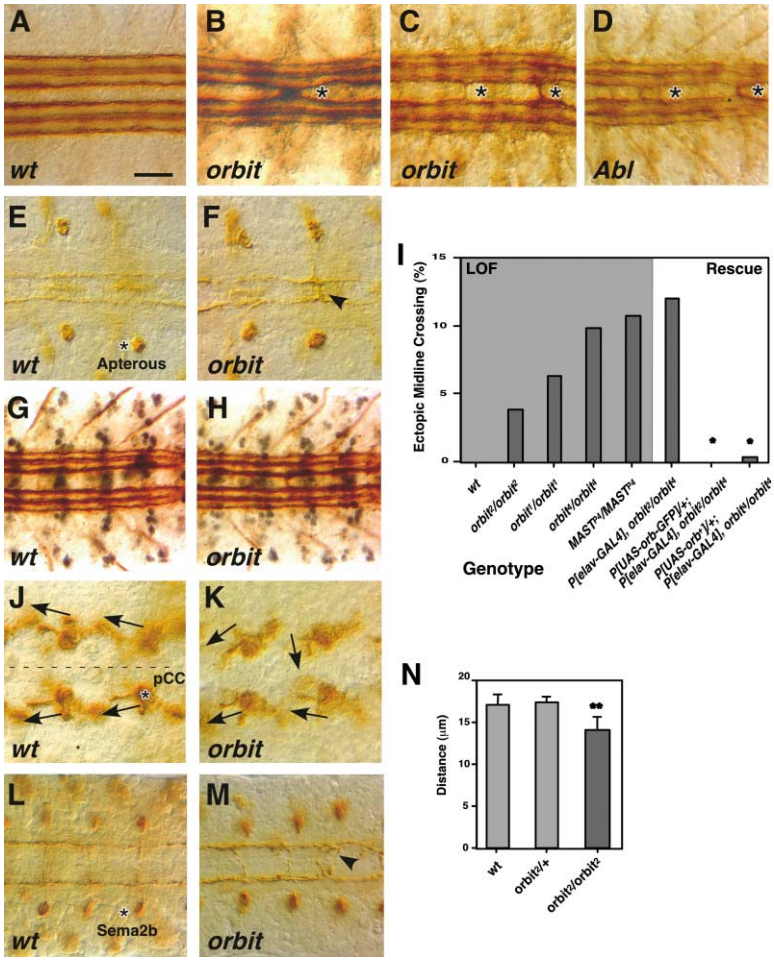

Figure 1. Orbit/MAST Is Required for Guidance and Lateral Position of CNS Axons

(A–D) Embryos of stage 17 were stained with m1D4 antibody and dissected. Ventral-down views are shown with anterior to left. The scale bar equals 8 μm. (A) In wild-type, three axon fascicles can be seen on each side of the midline. (B) In *orbit*^{1} mutants, medial axon fascicles merge (asterisk). (C) In *MAST*^{P4} mutants, axons abnormally cross the midline (asterisks). (D) The midline crossing defects (asterisks) of *Abl* mutants are identical to those of *orbit* mutants.

(E and F) Stage 17 embryos carrying a Tau-lacZ transgene under the apterous (Ap) promoter (ApC Tau lacZ) were stained with anti-LacZ antibody and dissected. (E) In wild-type, Ap neurons project their axons ipsilaterally and do not cross the midline. Asterisk indicates cell bodies of Ap neurons. (F) In *orbit*^{2} mutants, axons of Ap neurons abnormally cross the midline (arrowhead).

(G and H) Embryos of stage 17 were stained with anti-engrailed (blue) and m1D4 (brown). (G) In wild-type, subsets of midline and neuronal cells express engrailed. (H) In *orbit*^{4}, engrailed-expressing cells are present in normal numbers and positions, indicating that orbit mutations do not affect cell fate determination.

(I) Quantification of ectopic midline crossing is shown for an *orbit/MAST* allelic series (wild-type, n = 200 segments; *orbit*^{2}/*orbit*^{2}, n = 340; *orbit*^{1}/*orbit*^{1}, n = 240; *orbit*^{4}/*orbit*^{4}, n = 640; *MAST*^{P4}/*MAST*^{P4}, n = 410). A strong phenotype is rescued by panneuronal expression (*elav-GAL4*) of *orbit* cDNA transgenes (*P[elav-GAL4], orbit*^{2}/*orbit*^{4}, n = 100; *P[UAS-orbit*$^{+}$-GFP*];P[elav-GAL4], orbit*^{2}/*orbit*^{4}, n = 200; *P[UAS-orbit*$^{+}$*]; P[1407-GAL4], orbit*^{4}/*orbit*^{4}, n = 450).

(J) In wild-type, nascent posterior corner cell (pCC) pioneer axons extend anteriorly and ipsilaterally, slightly away from the midline. An asterisk and arrows indicate cell bodies and axon trajectories of individual pCC neurons, respectively; a dotted line indicates the midline.

(K) In *orbit* (*orbit*^{4}) mutants, pCC axons often orient toward the midline.

(L and M) Stage 17 embryos containing a *Tau-myc* transgene under the Semaphorin 2b promoter (Sema2b) were stained with anti-myc antibody and dissected. Asterisk indicates cell bodies of Sema2b neurons. (L) In wild-type, Sema2b neurons cross the midline in a straight vertical line before turning to follow a mediolateral axon fascicle. (M) In *orbit* mutants (*orbit*^{2}), Sema2b neurons exhibit erratic trajectories both approaching the midline (arrowhead) and along the longitudinal neuropil.

(N) Measurement of the distance between the left and right Sema2b fascicles reveals a highly significant inward shift in the lateral position of these axon tracts in *orbit*^{2}/*orbit*^{2} (double asterisks; n = 109) compared to wild-type and heterozygote controls (wild-type, n = 38; *orbit*^{2}/+, n = 52; $p < 0.01$; Student's t test).

quired cell autonomously during neuronal differentiation for accurate axon guidance decisions.

The late-stage axon pathway defects in *orbit/MAST* mutants suggest a failure in the repellent effects of Slit on growth cone orientation. To be certain that the *orbit/MAST* phenotype reflects a loss of growth cone orientation and not simply a change in patterns of axon fasciculation, we inspected axon trajectories of pioneer neurons before other axons were available to serve as a substrate for fasciculation. At late stage 12, the posterior corner cell (pCC) helps to pioneer the MP1 pathway proximal to the midline (Thomas et al., 1984); pCC neurites extend anteriorly and slightly away from the midline in wild-type (Figure 1J). In *orbit/MAST* homozygotes, we find that the pCC often orients toward the midline, sometimes crossing to meet its contralateral homolog (Figure 1K). This shows that Orbit/MAST is required for accurate directional specificity of axon growth.

In addition to controlling midline crossing of axons, Slit repulsion determines the lateral position of longitudinal axon fascicles within the CNS neuropil (reviewed by Rusch and Van Vactor, 2000). We used a marker for a mediolateral axon fascicle (Sema2b-Tau-myc; Rajagopalan et al., 2000) to examine this later function of Slit and its Robo receptors. In wild-type, Sema2b-positive axons cross the midline, turn, and extend along a straight longitudinal trajectory (Figure 1L). In *orbit/MAST* mutants, a few Sema2b-positive axons meandered toward the midline from lateral positions (Figure 1M). However, measurement of the lateral separation of these axon tracts reveals a significant inward shift in *orbit/MAST* mutants (Figure 1N; $p < 0.01$). Together, our ge-

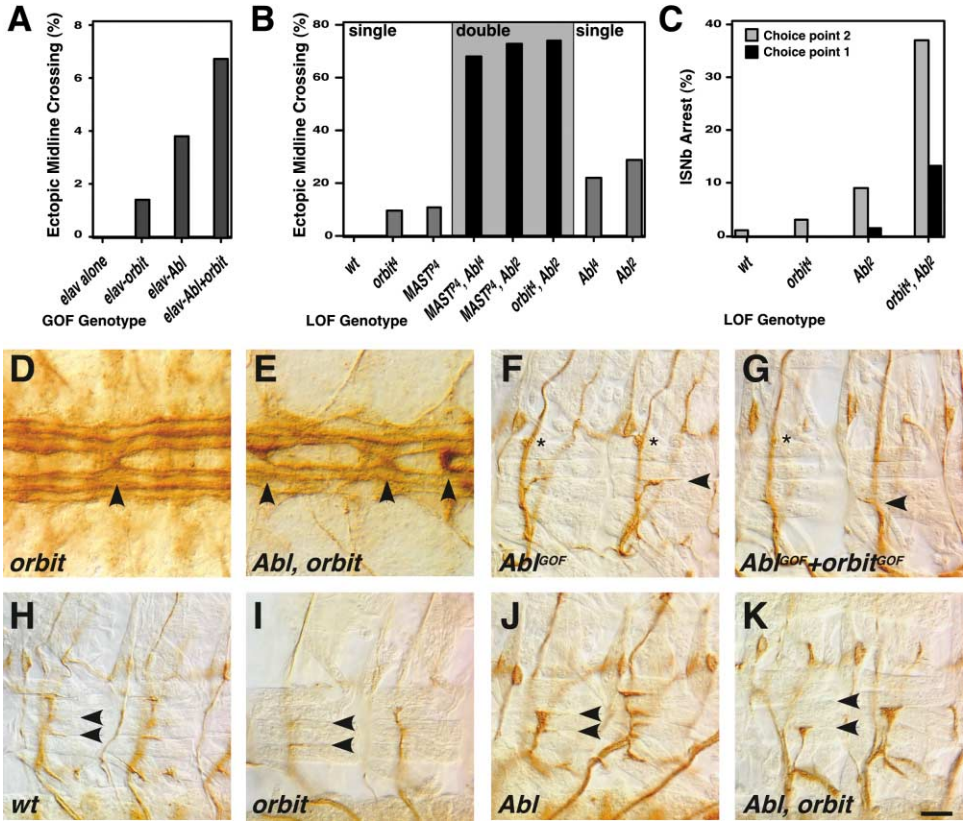

Figure 2. Orbit/MAST Cooperates with Abl during Axonal Development

(A) Overexpression of *orbit* (*EP3403*, n = 280) or *Abl* (*UAS-Abl*$^{+}$, n = 400) with an *elav-GAL4* driver causes errors in axon crossing at the midline assessed with anti-FasII staining. Embryos overexpressing *Abl* and *orbit/MAST* (n = 450) show a mild synergy at the midline.

(B) Loss of function in *orbit/MAST* or *Abl* causes ectopic midline crossing (wild-type, n = 200; *orbit*^{4}/*orbit*^{4}, n = 640; *MAST*^{P4}/*MAST*^{P4}, n = 410; *Abl*^{4}/*Abl*^{4}, n = 96; *Abl*^{2}/*Abl*^{2}, n = 102). A dramatic increase in midline crossing results from double loss of function of *orbit/MAST* and *Abl* (*MAST*^{P4}/*MAST*^{P4};*Abl*^{4}/*Abl*^{4}, n = 260; *MAST*^{P4}/*MAST*^{P4};*Abl*^{2}/*Abl*^{2}, n = 170; *orbit*^{4}/*orbit*^{4};*Abl*^{2}/*Abl*^{2}, n = 77), showing that the two genes cooperate during midline guidance.

(C) Strong synergy between *orbit/MAST* and *Abl* is also observed in the intersegmental nerve b (ISNb) growth cone arrest phenotype. The frequency of premature ISNb arrest increases dramatically in the double mutant (*orbit*^{4}/*orbit*^{4};*Abl*^{2}/*Abl*^{2}, n = 365), compared to the single homozygotes (wild-type, n = 108; *orbit*^{4}/*orbit*^{4}, n = 259; *Abl*^{2}/*Abl*^{2}, n = 279). In addition, the severity increases in the double mutant, where ISNb arrest is observed at both early (muscle 6/7; choice point 1) and late (muscle 13; choice point 2) choice points in the ventral domain (see arrows in [H–K]).

(D and E) The midline axon phenotype is much more severe in *orbit/MAST,Abl* double mutants compared to *orbit/MAST* (D) or *Abl* single mutants. Arrowheads indicate ectopic midline crossing.

(F) When *UAS-Abl*$^{+}$ is overexpressed with *elav-GAL4*, ISNb axons often fail to enter the ventral target domain (muscles 7/6, 13, and 12), leaving a subset of axons to innervate the targets (arrowhead). Once past their targets, the misguided ISNb axons often make contacts with muscle 12 ("reach-back"; asterisks).

(G) Coexpression of Abl and *orbit/MAST* under *elav-GAL4* slightly stronger phenotype.

(H) In wild-type, ISNb enters the ventral domain and passes through two choice points (arrowheads; muscle 6/7 and muscle 13; Van Vactor et al., 1993) before innervating muscle 12.

(I) ISNb arrest at the muscle 6/7 cleft can occasionally be found in *orbit* mutants (*orbit*^{4} is shown).

(J) The same ISNb phenotype is observed in *Abl* mutants (*Abl*^{2} shown).

(K) In *orbit/MAST,Abl* double mutants (*orbit, Abl*^{2} is shown), ISNb axons arrest more frequently at both choice points. Scale bar equals 5 μm.

netic data demonstrate that Orbit/MAST performs a cell-autonomous postmitotic function during growth cone navigation.

Orbit/MAST and Abl Cooperate during Axonogenesis

The interaction between Orbit/MAST and Abl in the retina predicted that these proteins might cooperate to mediate axon guidance choices. However, since Abl plays both positive and negative roles in Slit signaling (Bashaw et al., 2000; Wills et al., 2002; Hsouna et al., 2003), it was important to test the polarity of genetic interactions in the context of embryonic development. We first elevated Abl and Orbit/MAST levels alone or in combination in postmitotic neurons. We found a mild synergy between the two genes during midline guidance that is consistent with cooperation. Interestingly, overexpression of Orbit/MAST alone induces a low but significant number of guidance errors at the midline (Figure 2A). Stronger interactions were observed through LOF analysis. Double homozygous LOF mutants showed substantially increased ectopic midline crossing com-

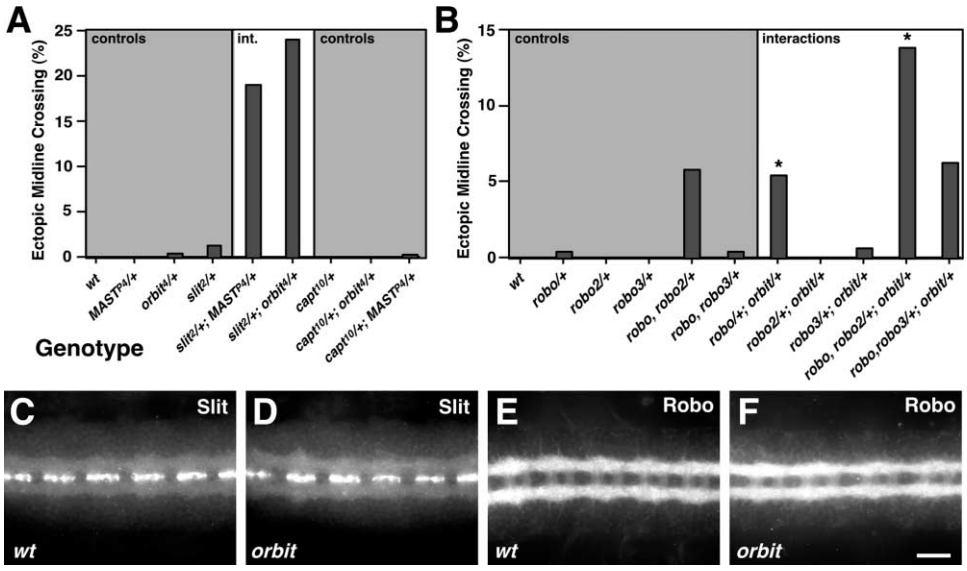

Figure 3. Orbit/MAST Displays Sensitive Interactions with Slit, Robo, and Robo2

(A) Embryos that are transheterozygous for both *orbit/MAST* and *slit*^{2} (white box; *slit*^{2}/+;*orbit*^{4}/+, n = 550; *slit*^{2}/+; *MAST*^{P4}/+, n = 670) show significant increase ($p < 0.01$) in ectopic midline crossing when compared to embryos that are heterozygous for single *orbit/MAST* or *slit* alleles (wild-type, n = 200; *MAST*^{P4}/+, n = 200; *orbit*^{4}/+, n = 520; *slit*^{2}/+, n = 720). As a control for the specificity of the interaction, embryos that are heterozygous for *capulet* (*capt*^{10}/+, n = 110) do not show any genetic interaction with *orbit/MAST* alleles (*orbit*^{4}/+;*capt*^{10}/+, n = 230; *MAST*^{P4}/+;*capt*^{10}/+, n = 370).

(B) Compared to controls (wild-type, n = 200; *robo*^{GA285}/+, n = 230; *robo2*^{8}/+, n = 200; *robo3*^{1}/+, n = 210; *robo*^{GA285},*robo2*^{8}/+,+, n = 190; *robo*^{GA285},*robo3*^{1}/+,+, n = 230), the midline crossing phenotype of *orbit*^{4} is significantly enhanced by a single allele of *robo* (asterisk; *robo*^{GA285}/+; *orbit*^{4}/+, n = 390; $p < 0.01$) but not *robo2*^{8} (n = 300) or *robo3*^{1} (n = 350). Heterozygosity in *robo2* causes an additional enhancement of *orbit/MAST* beyond the effect of *robo* alone (asterisk; *robo*^{GA285},*robo2*^{8}/+,+;*orbit*^{4}/+, n = 370; $p < 0.01$), but this is not true of robo3 (*robo*^{GA285}, *robo3*^{1}/+,+;*orbit*^{4}/+, n = 450), suggesting some specificity to receptor that is specialized for restricting midline crossing.

(C–F) Stage 17 wild-type and *orbit/MAST* null (*orbit*^{2}) homozygous embryos were live dissected, stained with anti-Slit or anti-Robo antibodies, and imaged with equal illumination and exposure times. Slit is expressed by midline glia and accumulates on axon surfaces within the neuropil in wild-type (C); Robo is localized to the surface of longitudinal axons in wild-type (E). Normal levels and localization are seen for Slit (D) and Robo (F) in *orbit*^{4} embryos.

pared to single mutant controls (Figures 2B and 2E), reminiscent of mutations in *robo* itself (Seeger et al., 1993). Due to large maternal contributions of Abl and Orbit/MAST (Inoue et al., 2000; Lemos et al., 2000; Grevengoed et al., 2001; Maiato et al., 2002), even amorphic alleles are not zygotic null. Thus, it is not possible to use the double LOF mutant to conclude that both proteins act in a common pathway; however, the observed synergy does show that Abl and Orbit/MAST cooperate during midline axon guidance.

Since Abl is also required for motor axon pathfinding in the periphery (Wills et al., 1999a), we compared inter-

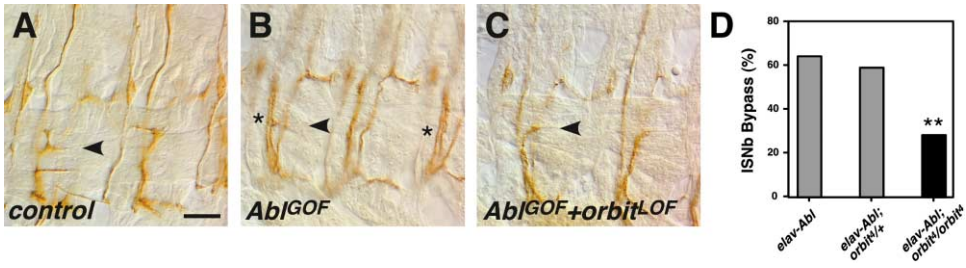

Figure 4. Orbit/MAST Is Required for Abl Kinase Function during Axon Guidance

(A) In late-stage embryos expressing *elav-GAL4* alone, ISNb innervates the clefts between muscles 6 and 7 and 13 (arrowhead) and 12 normally. The scale bar equals 8 μm.

(B) In embryos overexpressing Abl (*P[elav-GAL4],P[UAS Abl*$^{+}$*]*), ISNb fails to innervate its target muscles and instead follows ISN (asterisks mark the ISNb bypass phenotype in the ISN focal plane).

(C) The ISNb bypass phenotype of *Abl* GOF is suppressed in *orbit/MAST* LOF mutants (*P[elav-GAL4], orbit*^{4}*/P[UAS Abl*$^{+}$*], orbit*^{4}). This embryo has a normal innervation on muscle 13 (arrowhead) but still lacks an innervation on muscle 12.

(D) Quantification of the ISNb bypass phenotype in the genotypes shown in (A)–(C) reveals that bypass is significantly decreased ($p < 0.01$, double asterisk) in embryos with reduced *orbit/MAST* activity compared to *Abl* GOF alone (*P[elav-GAL4],P[UAS Abl*$^{+}$*]*, n = 81; *P[elav-GAL4], orbit*^{4}*/P[UAS Abl*$^{+}$*], +*, n = 172; *P[elav-GAL4], orbit*^{4}*/P[UAS Abl*$^{+}$*], orbit*^{4}, n = 236).

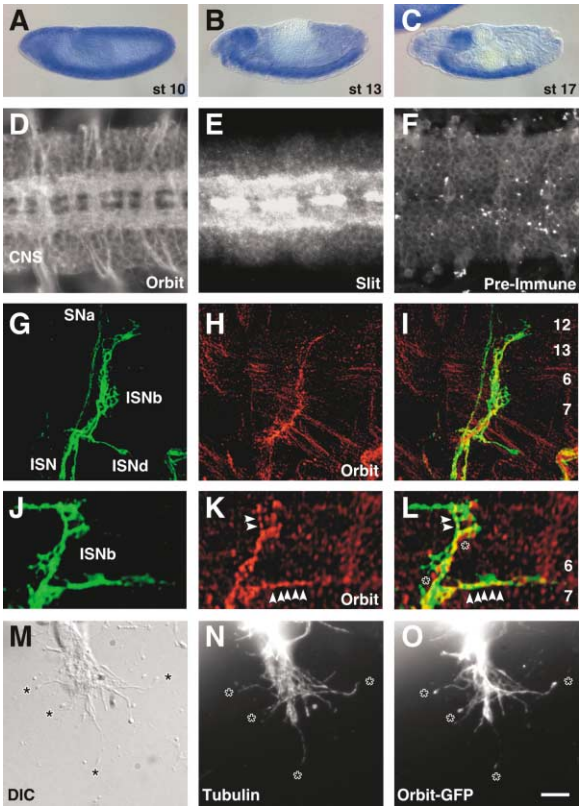

Figure 5. Orbit/MAST Localizes to *Drosophila* Embryonic Axons and Growth Cones

(A–C) *orbit/MAST* in situ hybridization on wild-type embryos is shown at mid and late stages: *orbit/MAST* is expressed in a broad pattern at stage 10 and before (A); however, this expression becomes restricted to the nervous system (ventral nerve cord and central complex) at later stages (stage 13 in [B]; stage 17 in [C]). (D–F) Wild-type embryos of stage 17. Orbit protein predominantly localizes to the CNS axons, accumulating on longitudinal, commissural, and exiting neuropil (D). In the same embryo and focal plane, anti-Slit antibodies highlight the midline glia and the accumulation of secreted Slit on the neuropil surface (E). In control embryos, preimmune sera label soma but not axons (F). (G–I) Wild-type embryos were stained with anti-FasII (mAb 1D4; green) and anti-Orbit (red) antibodies, imaged by confocal and Z-stack projections that were generated. SNa, ISN, ISNb, and ISNd motoneuron pathways are shown (G) as they grow past the ventral muscles (numbered in [I]). Orbit protein accumulates in the growth cones of ISNb within the ventral target domain (H), showing less accumulation within the ISNb axons as they approach the targets ([I] shows the merged image of [G] and [H]; yellow indicates the Orbit signal that is contained within the motor growth cones. Note: a 3D rendered movie of this confocal stack is included in the Supplemental Materials at http://www.neuron.org/cgi/content/full/42/6/913/DC1). Orbit also accumulated in the ventral muscles (H). (J–L) Higher-magnification views of another ISNb nerve (J) within its target domain show that Orbit (K) is distributed in puncta along the axon and within the growth cones (indicated by arrowheads in [K]). Orbit is also localized outside the axons, within the muscle, near points of nerve contact (asterisks; muscles 6 and 7 are labeled). ([L] shows the merged image of [J] and [K].) (M–O) Stage 16 embryonic CNS explants expressing orbit-GFP with an *elav-GAL4* driver were cultured on glass coverslips (see the Experimental Procedures). Axons and growth cones (asterisks) can be seen in differential interference contrast (DIC in [M]), for comparison to staining with anti-Tubulin (Sigma mAbDM1A) (N) or Orbit-GFP (O). Orbit localizes along the axons and accumuates in the growth cones. Scale bar equals 120 μm in (A)–(C), 15 μm in (D)–(F), 4 μm in (G)–(I), 2 μm in (J)–(L), and 10 μm in (M)–(O).

segmental nerve b (ISNb) morphology in double and single mutants. Overexpression of Abl generates an ISNb bypass phenotype where this group of axons fail to enter their target domain (Wills et al., 1999b; Figure 2F). Coexpression of Abl and Orbit/MAST does enhance the expressivity of phenotype slightly (e.g., Figure 2G), but the effect is subtle. Once having entered the ventral target domain, wild-type ISNb axons innervate the clefts between muscles 6, 7, 12, and 13 (Figure 2H). In *Abl* LOF mutants, ISNb stops short of its final targets, often terminating at muscle 13 (Wills et al., 1999a; Figure 2J). We observed a similar ISNb growth cone arrest phenotype at very low penetrance in *orbit/MAST* LOF alleles (Figure 2I). However, comparison of these phenotypes to *orbit,Abl* recombinant homozygotes revealed a strong enhancement of ISNb arrest in double LOF mutants, increasing the frequency of defects and shifting arrest to a more proximal position at the muscle 6/7 cleft (Figures 2C and 2K). Thus, Abl and Orbit/MAST cooperate during axon guidance decisions in multiple contexts.

Orbit/MAST Interacts with Slit and Multiple Roundabout Receptors

Our analysis of CNS axons suggested that Orbit/MAST is an effector in the Slit/Robo repellent pathway. To test the hypothesis, we turned to the same genetic assay that was used to identify Slit as the ligand for the Robo receptor family (Kidd et al., 1999). While heterozygotes lacking one copy of Slit or its receptors show very few guidance errors at the midline choice point, transheterozygotes that also remove one copy of a second gene in the pathway often reveal strong, synergistic phenotypes. Indeed, while *orbit/MAST* heterozygotes show no significant midline defects, very strong synergy is observed with mutations in *slit* (roughly 10-fold; Figure 3A). As a control for the specificity of the interaction, we examined embryos lacking different alleles of *orbit/MAST* and an allele of *capulet* (*capt*), an actin binding protein that shows strong interactions with both *slit* and *Abl* (Wills et al., 2002). No synergy was observed between *capt* and *orbit/MAST* (Figure 3A). We then performed the same transheterozygote analysis with single mutations in the repellent receptors; we found that *orbit/MAST* enhanced *robo* (Figure 3B). Additional crosses revealed that *orbit/MAST* interacts with *robo* and *robo2* but not with *robo3* (Figure 3B, see legend), consistent with the specialization of Robo and Robo2 for midline crossing (reviewed by Rusch and Van Vactor, 2000). To be certain that Orbit/MAST is not required simply for the expression or delivery of Slit and/or Robo protein, we compared staining in wild-type and *orbit/MAST* embryos, but saw no obvious differences (Figures 3C–3F).

Orbit/MAST Is Epistatic to the Abl Kinase

While all our data supported the model that Orbit/MAST is necessary for Abl function during axon guidance, we wanted a more rigorous test. If Orbit/MAST acts as an effector of Abl, we would also expect *orbit/MAST* mutations to be epistatic to an *Abl* GOF phenotype. The fact that Abl acts in both positive and negative capacities during midline guidance complicates the interpretation of such an experiment within the CNS; however, Abl plays a less complex role for ISNb motor axons (Wills

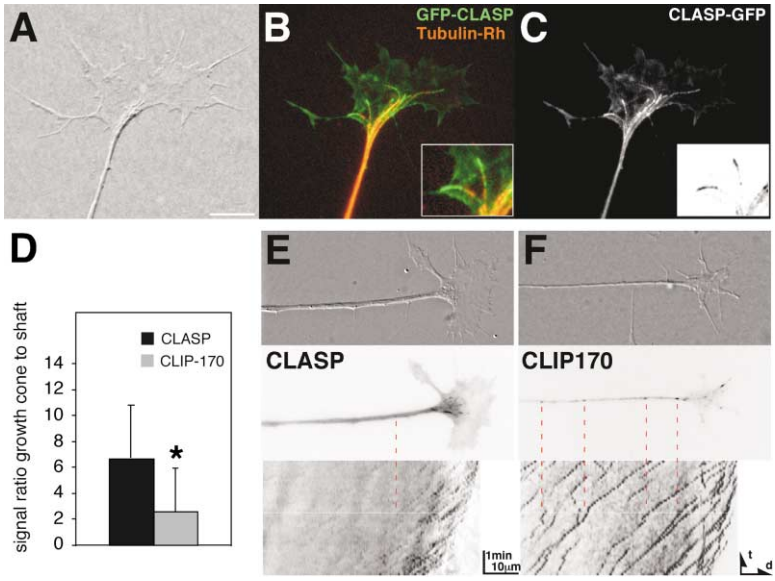

Figure 6. Localization of GFP-CLASP in *Xenopus* Growth Cones

(A–C) GFP-CLASP expression in a growth cone reveals CLASP localization to plus ends of microtubules labeled with Rhodamine-Tubulin ([A] shows DIC image; [B] shows dual channel). The signal is most intense at the microtubule tip ([B] inset), while lower levels are detected along the length of microtubules (GFP-CLASP alone in [C]; inset shows GFP-CLASP signal intensity inverted). (D) Enrichment of CLASP in growth cones. To calculate the ratio of GFP signal between growth cone and shaft for CLIP and CLASP, the dashes detectable in 50 μm shaft and in the growth cones were counted every 10 s and averaged over 3 min. The ratio for GFP-CLASP-expressing neurons ($n = 4$) is significantly higher ($p = 0.001$) than the ratio in GFP-CLIP-170-expressing neurons ($n = 5$). (E and F) Kymographic analysis (see the Experimental Procedures) of GFP-CLASP and GFP-CLIP-170 dynamic localization in growth cones. DIC images above provide context. Dashed lines show position of individual GFP-positive dashes at the time point represented in the middle panel (this corresponds to the white horizontal line in the kymograph below). (E) In a GFP-CLASP-expressing axon, GFP dashes are detected primarily in the growth cone, while dashes in the shaft are few and low in intensity. (F) GFP-CLIP-170 confirms microtubule plus end tracking behavior in the growth cone and axon shaft (Stepanova et al., 2003). The average velocity of GFP-CLIP-170 dashes in the shaft is 6.9 μm/min. Scale bar equals 10 μm (A); inset (B and C) is 10 μm wide.

et al., 1999b). When overexpressed under a strong post-mitotic neural GAL4 source, Abl generates an ISNb bypass phenotype (Figures 4B and 4D; neuronal expression of GAL4 alone has no effect; Figure 4A). However, when Abl is overexpressed in an *orbit/MAST* homozygous background, the frequency of ISNb bypass drops approximately 2-fold (Figures 4C and 4D). This indicates that Orbit/MAST acts genetically downstream of Abl in embryonic growth cones.

Orbit/MAST Localizes to Axons and Growth Cones

If Orbit/MAST plays a direct role in axonal navigation, we would expect the protein to localize within growth cones. Previous characterization of Orbit/MAST expression focused on cell division; however, no description of Orbit/MAST expression in differentiating neurons exists. Using in situ hybridization, we asked if *orbit/MAST* is transcribed in the CNS during the late embryonic stages when axon pathways are constructed. At early stages of development, *orbit/MAST* RNA expression is quite broad (e.g., Figure 5A). However, during the key stages of neuronal differentiation (stages 12 through 17), we find that the signal accumulates in the developing CNS (Figures 5B and 5C).

To investigate localization of endogenous protein, we used anti-Orbit/MAST antibodies on the embryonic CNS and found that it accumulates largely within the neuropil (Figures 5D–5F), consistent with localization within axons and growth cones. To obtain higher-resolution images of growth cones that require Orbit/MAST, we examined motor growth cones visualized with the membrane marker FasII (Van Vactor et al., 1993). Orbit/MAST localized along motor axon shafts as they extend through the periphery (Figure 5G–5I). Although Orbit/MAST was also expressed in embryonic muscles (Figure 5H), three-dimensional reconstruction of confocal images after deconvolution shows that a substantial amount of Orbit/MAST is contained within the growth cone perimeter as defined by Fas II (Figures 5J–5L, arrowheads). Interestingly, mesodermal Orbit/MAST puncta seemed to be most intense at sites of motor nerve contact (Figure 5L, asterisks).

To confirm that Orbit/MAST accumulates in growth cones, we expressed an Orbit/MAST-GFP fusion protein in neurons (see Figure 5 legend). This construct fully rescues the *orbit/MAST* mutant defects (Figure 1). We then made explants of the transgenic CNS and grew axons alone on a glass substrate (see the Experimental Procedures). In this assay, Orbit/MAST localized along the axon and accumulated at the expanded tips of processes, correlating with the distal ends of axonal microtubules (Figures 5M–5O). Taken together, these findings demonstrate that Orbit/MAST protein is in the right location to play a direct role in growth cone turning. However, due to the small size of *Drosophila* growth cones, high-resolution images of Orbit/MAST subcellular localization and dynamics are difficult to obtain in this system. Thus, we turned to larger vertebrate growth cones for the next level of analysis.

Vertebrate CLASP Identifies a Subset of Growth Cone Microtubule Plus Ends

The vertebrate Orbit/MAST ortholog CLASP is known to localize along microtubules and at their plus ends in nonneuronal cells (Akhmanova et al., 2001); however, its behavior in vertebrate growth cones is unknown. We used GFP-CLASP fusion proteins that were expressed in developing *Xenopus* spinal cord neurons to examine CLASP localization and dynamics. GFP-CLASP accumulated in comet-shaped dashes that localized to the tips of microtubules labeled with Rhodamine-conjugated Tubulin subunits in motile growth cones (Figure

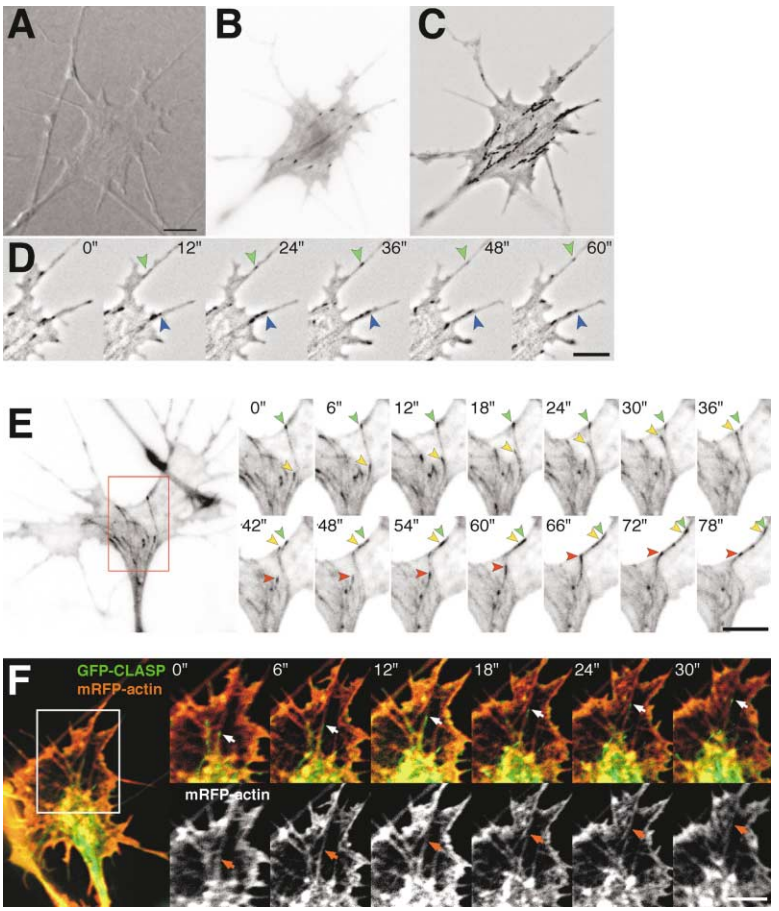

Figure 7. GFP-CLASP-Positive Microtubules Interact with Actin-Rich Periphery

(A–D) Invasion of GFP-CLASP-positive microtubule plus ends into growth cone filopodia. (C) An overlay of multiple time points reveals tracks of microtubule plus ends moving into filopodia (maximum projection of 14 frames spanning 72 s). (D) Time lapse showing microtubule plus ends (green and blue arrows) penetrating into the base of filopodia. (E) GFP-CLASP-positive microtubules grow toward the leading edge. In the inset time series (red box defines expanded area for inset), three dashes (arrows) follow the same track and buckle as they grow along the membrane. Note that the microtubule that is highlighted by the green arrowhead pauses for 30 s without losing GFP-CLASP association before resuming growth. (F) Growth cone expressing GFP-CLASP and mRFP1-actin (monomeric red fluorecent protein-1-actin). In the inset time lapse, a microtubule tracking along an actin bundle for 30 s is highlighted by a white arrow. The lower panel shows mRFP1-actin to visualize actin bundles extending into filopodia. Elapsed time is indicated in seconds in the upper corner of each inset panel. Scale bars equal 5 μm.

6B). Lower levels of GFP-CLASP were also seen along the length of microtubules (Figure 6C) and diffusely in the cytoplasm. When the numbers of CLASP-positive dashes were compared in growth cones and axon shafts, it was evident that CLASP was preferentially localized to the growth cone (Figures 6D and 6E; for Quicktime movies of these and other imaging data, see the Supplemental Data at http://www.neuron.org/cgi/content/full/42/6/913/DC1), consistent with a function specialized for axon growth or navigation. Another plus end tracking protein, CLIP-170, showed far less preference for the growth cone (Figures 6D and 6F) and highlighted the presence of microtubule plus end growth along the axon shaft (see kymograph at bottom of Figure 6F), as reported for CLIP-170 and EB-3 in Purkinje cells (Stepanova et al., 2003). These findings suggest that CLASP identifies a subset of microtubules within the growth cone.

The CLASP and CLIP-170 dashes both exhibited movement predominantly toward the growth cone leading edge (see kymographs in Figures 6E and 6F). Consistent with growing plus end tracking behavior, GFP-CLASP dashes moved at an average of 9.7 ± 2.1 μm/min, matching previously recorded microtubule growth rates in *Xenopus* neurons (10.5 ± 1.9 μm/min; Tanaka and Kirschner, 1991). Microtubules that underwent catastrophe and retracted lost their GFP-CLASP signal. Thus, the Orbit/MAST/CLASP protein associates preferentially with dynamic microtubule domains.

Further imaging of GFP-CLASP dynamics revealed that CLASP identifies a subset of microtubules that probe and penetrate the growth cone leading edge where guidance signals influence actin assembly. Tracking of individual GFP-CLASP dashes showed that some of the microtubule plus ends that accumulate CLASP extend into individual filopodia (Figures 7A–7D; overlay of many time points in Figure 7C illustrates the progressive movement into several filopodia). Often, several microtubule plus ends were observed to follow the same path (Figure 7E), as if guided by actin structures in the periphery. Interestingly, we could see GFP-CLASP-positive microtubules bend and pause and then conform to a novel path as they entered the growth cone periphery (inset, Figure 7E), as was previously described for pioneer microtubules interacting with actin filaments in the growth cone (Schaefer et al., 2002). Indeed, when we imaged actin and GFP-CLASP simultaneously, we could see microtubules track along actin bundles emanating from individual filopodia (Figure 7F). Together, these data indicate that CLASP localizes to the subcellular domain, where microtubule advance into the leading edge is controlled.

Elevated CLASP Impedes Growth Cone Microtubule Advance

The localization of CLASP to a subset of microtubule plus ends that explore the growth cone periphery supports the model that CLASP activity directly mediates

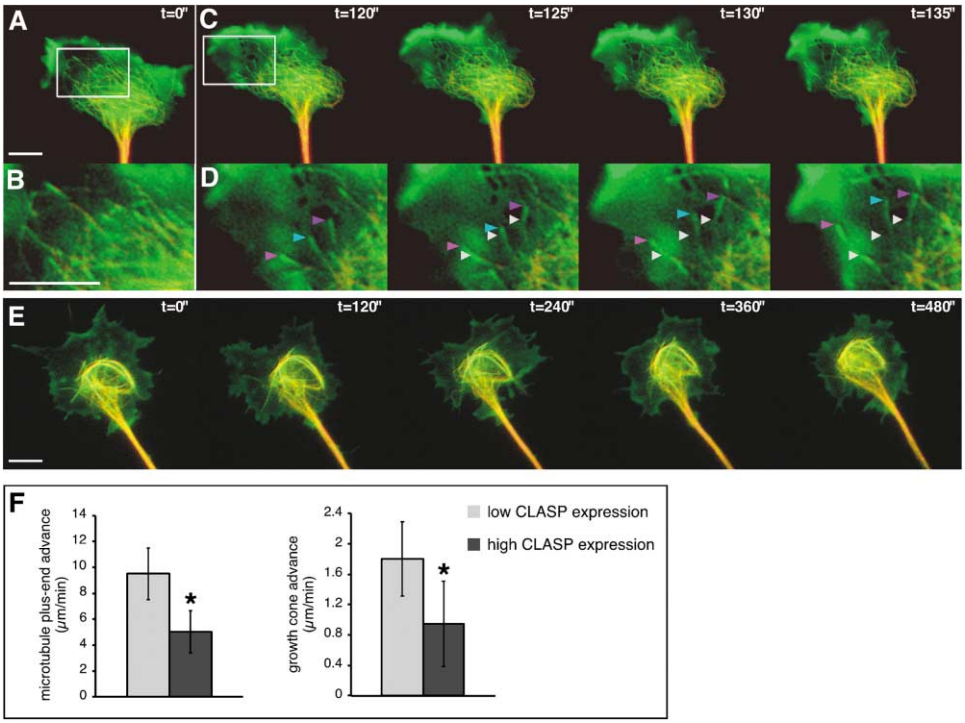

Figure 8. Increased CLASP Causes Looping and Decreased Growth of Microtubules

(A) Dual-channel image shows GFP-CLASP (green) and Rhodamine-Tubulin (red) at low levels of fusion protein expression (see text) at the beginning of a time series. Inset shows higher-magnification view in which individual microtubules and GFP-positive dashes can be tracked for relative position and growth. (C) Consecutive frames of a time-lapse movie (time in seconds is shown in upper right corner of each panel) are shown in sequence, with the positions of three microtubule plus ends marked (colored arrowheads), relative to their original positions (white arrowheads) at t = 120 s (D). (E) A longer time-lapse sequence shows the microtubule morphology and growth cone dynamics at high levels of GFP-CLASP fusion protein expression. Note that the time series in (E) is longer than that shown in (A) and (C); however, there is less forward movement of the growth cone. (F) Quantitative analysis of microtubule plus end advance rates and growth cone advance comparing neurons with low (n = 7) and high (n = 6) GFP-CLASP expression levels. Only growth cones that still showed some degree of plus end dynamics were included in this analysis (e.g., not the growth cone shown in [E]). This analysis shows that increased CLASP activity induces a 2-fold reduction in plus end extension ($p = 0.001$) and is correlated with a reduced growth cone advance ($p = 0.015$). Scale bar equals 5 μm.

an important part of the repellent response. However, the finding that elevated CLASP activity stabilizes microtubules in nonneuronal cells (Akhmanova et al., 2001) raised the question of how microtubule stabilization might contribute to repulsion of the leading edge. While CLASP LOF was not possible in *Xenopus* neurons where we could examine microtubule dynamics and morphology in detail, we decided to explore this question by elevating CLASP activity. Using mRNA injection to control the amount of GFP-CLASP expression, we found that low levels had no effect on the morphology or dynamics of growth cone microtubules (Figures 8A–8D). However, high levels of GFP-CLASP correlated with several striking observations. In these growth cones (Figure 8E), microtubules failed to extend beyond the transition zone and instead were found looping back into the C domain. Such microtubule looping has been noted in paused growth cones (reviewed by Kalil et al., 2000).

However, the most surprising feature came from a quantitative analysis of the rates of microtubule extension. For this, CLASP-expressing neurons were grouped into low-expressing neurons and compared to high-expressing neurons that still showed some degree of microtubule dynamics. We found that microtubule advance was significantly slower in growth cones with high CLASP expression (Figure 8F). This correlated with a reduced leading edge advance in growth cones displaying high CLASP-GFP expression (Figure 8F; compare also time courses in Figures 8A and 8E). Thus, CLASP can impede microtubule growth toward the leading edge and cause the growth cone to slow down. This supports our genetic data that place CLASP downstream of a growth cone repellent.

Discussion

Growth cone navigation relies on the induction of cell polarity events at the motile leading edge through intracellular signaling downstream of asymmetrically distributed guidance cues. Although microtubule dynamics have been long appreciated as important for guidance behavior, and several MAPs have been implicated in general axonogenesis, pathways that link such effector proteins to specific receptors have been elusive (reviewed by Dent and Gertler, 2003; Gordon-Weeks, 2004). Here, we describe the identification of Orbit/Chb/MAST/CLASP (hitherto described as CLASP) as a partner of the Abl tyrosine kinase in Slit-mediated growth cone repulsion. While previous studies of CLASP family proteins in nonneuronal cells revealed functions for

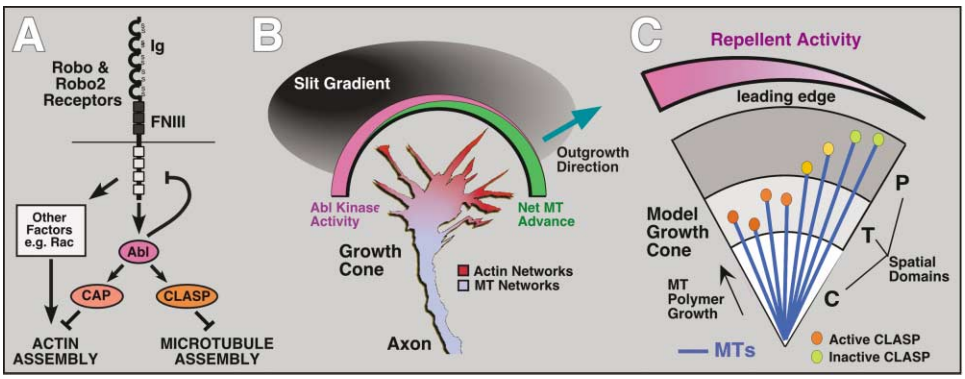

Figure 9. A Model for Orbit/MAST/CLASP Function during Growth Cone Orientation

(A) Genetic data indicate that Abl catalysis is required for the repellent activity of Robo receptors in response to the ligand Slit (Wills et al., 2002; Hsouna et al., 2003), while also providing negative feedback to downregulate Robo function and/or localization (Bashaw et al., 2000). As part of the downstream repellent response, which certainly includes other signaling factors, such as the GTPase Rac, that help to control actin assembly (e.g., Fan et al., 2003), Abl cooperates with multiple effectors, including the actin binding protein Capulet (Capt; Wills et al., 2002) and Orbit/MAST/CLASP (this study), suggesting that Abl simultaneously coordinates the dynamics of two major cytoskeletal systems to achieve growth cone repellent guidance. (B) We propose that an asymmetric distribution of Slit induces an internal asymmetry of Abl kinase activity. Since Orbit/MAST/CLASP activity is necessary for repulsion and cooperates with Abl in vivo, we also propose that its activation by Abl acts to impede growth cone advance nearest the source of Slit, likely by shifting net microtubule extension (green) and thus the outgrowth direction (turquoise arrow) away from higher levels of the repellent factor. (C) A model growth cone is faced with a gradient of repellent signaling at the leading edge (purple). A fan of microtubules (blue lines) extend from the central ("C") domain to the transitional ("T") domain to the actin-rich peripheral ("P") domain. In response to high levels of repellent signaling, Orbit/MAST/CLASP (small circles) is activated (orange circles) and acts to impede microtubule extension and leading edge advance near the source of the repellent factor, allowing the growth cone to move forward in the direction of low repellent signaling and low Orbit/MAST/CLASP activation (green circles).

these microtubule effector proteins in mitotic spindle dynamics and cell motility (reviewed by Maiato et al., 2003), their role in neurons has been unknown until now.

Our genetic analysis reveals a postmitotic requirement for CLASP during the guidance of axons in multiple contexts. At the midline, we find that CLASP is necessary for accurate growth cone orientation away from the source of Slit and for lateral positioning of longitudinal axon fascicles, suggesting a model in which CLASP acts positively downstream of Abl as part of the repellent response initiated by activation of Roundabout receptors. Genetic interaction and epistasis experiments support this model. Moreover, protein localization studies in *Drosophila* and *Xenopus* growth cones indicate that this role for CLASP is likely to occur near the leading edge, where guidance cues exert their initial influence on cytoskeletal remodeling. In contrast to CLIP-170, CLASP is enriched at microtubule plus ends within the growth cone itself, suggesting a specialized role in neuronal cell biology. Indeed, CLASP-positive plus ends penetrate the growth cone peripheral domain and track along microfilament bundles into individual filopodia proximal to the site of guidance receptor activation. Taken together, the genetics and cell biology suggest a model in which Slit activation of the Abl kinase leads to a CLASP-dependent inhibition of microtubule extension favoring growth cone advance toward regions of low signaling activity (see below).

Abl Coordinates Multiple Cytoskeletal Effector Systems

Growth cone repellents play a major role in patterning neuronal connectivity and restricting regenerative capacity within the CNS (reviewed by Schwab, 2000; Dickson, 2002), making repellent signaling a high priority for functional dissection. One theme to emerge from many studies of growth cone guidance is that the cell biology of directional navigation requires a coordination of many different subcellular events (reviewed by Lee and Van Vactor, 2003). This predicts the existence of signaling proteins that can regulate the combined activities of multiple effectors. Receptor-proximal factors fitting this profile have been found in several repellent pathways. For example, the guanine-nucleotide exchange factor Ephexin mediates EphA4-dependent repulsion by activating RhoA and simultaneously inhibiting Rac and Cdc42 (Shamah et al., 2001). The adaptor protein Grb4 displays coordinate interactions with a different cast of players downstream of Ephrin-B, including the kinase Pak1, the Cbl-associated protein (CAP/Ponsin), and the Abl-associated protein-1 (Abi-1), highlighting the diversity of potential effectors (Cowan and Henkemeyer, 2001).

Through genetic analysis in *Drosophila*, the Abl tyrosine kinase has emerged as another key signaling center that is capable of coordinating multiple outputs (reviewed by Moresco and Koleske, 2003). Abl is both necessary and sufficient to define axon guidance behavior (e.g., Wills et al., 1999a, 1999b, 2002; Bashaw et al., 2000; Hsouna et al., 2003), suggesting that it acts high in the signaling hierarchy. At the CNS midline, Abl interacts with Enabled and the cyclase-associated protein (Capulet) to control growth cone behavior (Bashaw et al., 2000; Wills et al., 2002). These Abl effectors are actin binding proteins with different types of activity in cytoskeletal dynamics (reviewed by Lee and Van Vactor, 2003). Abl is also likely to regulate β-Catenin/Armadillo function (Loureiro and Peifer, 1998), which may be important for the in vivo response to Slit (Rhee et al., 2002). While many studies on the cell biology of Abl family kinases

have focused on actin effectors and Abl's ability to bind directly to actin polymers, recent work reveals that the Abl-related gene (Arg) associates directly with microtubules as well, thus placing it at the interface between the two cytoskeletal arrays (Miller et al., 2004). Our genetic screen and analysis of CLASP function in *Drosophila* adds a new dimension to this picture, showing that Abl controls both actin and MAPs in parallel (Figure 9A).

CLASP and Growth Cone Microtubule Dynamics

CLASP family proteins fall into an intriguing group of microtubule-associated plus end tracking proteins (+TIPs; reviewed by Carvalho et al., 2003). While little is known about their function in neurons, and their precise mechanism of action is still mysterious, accumulated evidence suggests that +TIPs act to regulate microtubule stability. For example, dominant-negative experiments with CLIP-170 in nonneuronal cells suggest that this +TIP acts to reduce the frequency of rapid microtubule depolymerization (or "catastrophe"; Komarova et al., 2002). While the impact of CLASP family function has not been determined using dynamic assays, overexpression of CLASP in COS cells increased the number of stabilized microtubules (Akhmanova et al., 2001). Preliminary RNA interference to remove CLASP in *Drosophila* S2 cells indicates that this function has been conserved (A. Ghose, U.E, and D.V.V., unpublished data). However, if an increase in stable microtubules comes at the expense of dynamic microtubule segments, then we might predict a negative impact on the persistence of growth cone advance, based on existing pharmacological data (e.g., Tanaka et al., 1995; Dent and Kalil, 2001; Buck and Zheng, 2002). This provides an attractive model to explain how CLASP can cooperate with Slit, Robo, Robo2, and Abl during midline repulsion.

A growing number of MAPs have been shown to localize to plus ends (reviewed by Carvalho et al., 2003), raising the possibility that +TIP protein complexes coordinate multiple activities. In addition to the CLASP localization in this study, the EB1 family member EB3 displays +TIP behavior within the growth cone (Stepanova et al., 2003). Interestingly, the +TIPs EB1 and APC associate with Short stop/Kakapo/MACF in *Drosophila* cells (Subramanian et al., 2003). Short stop is known to bind both actin and microtubule polymers, suggesting a role in mediating interactions between the two polymer networks (e.g., Lee and Kolodziej, 2002). Moreover, *short stop* mutants display an ISNb motor axon phenotype that is nearly identical to *orbit/MAST* and *Abl* loss of function (Van Vactor et al., 1993). Other MAPs have also been implicated in mediating interaction between microfilaments and microtubules in developing axons (reviewed by Dehmelt and Halpain, 2004), suggesting that this interface will be complex and highly coordinated. Future experiments will address whether other +TIP-associated proteins also contribute to repellent signaling and whether all the +TIP proteins display similar activities in vivo.

A Model for the Mechanism of Slit-Mediated Growth Cone Turning

With a combination of in vivo genetic analysis and dynamic imaging, we can propose a working model for the role of CLASP in growth cone repellent signaling. Recent work indicates that Abl functions positively to support Slit/Robo-mediated axon repulsion at the midline (Wills et al., 2002; Hsouna et al., 2003). This suggests a model in which the polarity of cytoskeletal advance within the growth cone reflects an asymmetry of Abl kinase activity in response to a graded distribution of Slit. Since multiple lines of genetic evidence show that CLASP cooperates with Abl and acts genetically downstream of the kinase, we favor a model where CLASP helps to induce cytoskeletal events that are needed to impede leading edge advance nearest the source of Slit (purple in Figure 9B), thus allowing relative advance at sites most distant from the source (green in Figure 9B). This model predicts that elevation of CLASP activity will have a negative impact on growth cone extension and on microtubule advance. Our *Xenopus* overexpression experiments satisfy this prediction (Figure 8).

Since the entire growth cone perimeter must remain competent to respond to asymmetrically localized repellents in order to navigate through complex terrain, we anticipate that CLASP activity rather than its localization will change in response to local kinase activation. Studies of the actin regulatory protein mammalian Enabled (Mena), which localizes to the tips of filopodia, suggest an analogous mechanism downstream of cyclic nucleotide-gated kinases to control filopodium formation (Lanier et al., 1999; Loureiro et al., 2002; Lebrand et al., 2004). Abl regulates both CLASP and Enabled during axon guidance in *Drosophila* (Wills et al., 1999a; Bashaw et al., 2000; this study), suggesting that independent cytoskeletal effectors must be coordinated to achieve accurate navigational choices. In this regard, it will be interesting to ask how CLASP interacts with key factors like the GTPase Rac1, which appears to be important in midline guidance (e.g., Fan et al., 2003) and interfaces with CLIP-170 in nonneuronal cells (Fukata et al., 2002a). While many assume that the immediate effectors in axon guidance are actin regulators, data from nonneuronal systems suggest that microtubule dynamics can control actin assembly from the inside out (reviewed by Rodriguez et al., 2003).

Experimental Procedures

Additional methodological detail and references can be viewed in the Supplemental Experimental Procedures at http://www.neuron.org/cgi/content/full/42/6/913/DC1.

Genetic Strains, Crosses, and Manipulation

Hypomorphic *orbit* alleles *orbit*^{1} and *mast*^{p4} and null *orbit* alleles *orbit*^{2} and *orbit*^{4} were obtained from Drs. C. Sunkel and D. Glover. *Abl, slit, capt, robo, robo2, and robo3* alleles that were used were previously described (Wills et al., 2002). To identify homozygous embryos of the alleles above, *TM6B Ubx-lacZ, CyO wg-lacZ, CyO actin5C-LacZ, and TM6B ubi-GFP* balancers were used (provided by Drs. K. Zinn, B. Dickson, and T. Schwarz). For double mutant analyses, *orbit* and *Abl* alleles were combined using *ri* and *st* as markers. To analyze the behavior of identified neurons in *orbit* mutants, third-chromosome insertions of *Semaphorin (Sema)2b-Tau-myc* (provided by Dr. B. Dickson) or *Apterous-Tau-lacZ* (*ApC Tau lacZ*; provided by Dr. S. Thor) were combined onto *orbit*^{2} or *orbit*^{4} chromosomes. For gain-of-function analyses, a postmitotic, neuron-specific driver, *elav-GAL4*, was used to direct expression of *UAS-Abl*$^{(+)}$ and an *orbit* EP line (EP 3403).

Constructs and RNA

Fusions of enhanced green fluorescent protein with human CLASP2γ (GFP-CLASP) and rat CLIP-170 (GFP-CLIP-170) were obtained from Dr. N. Galjart (Akhmanova et al., 2001) and cloned into pCS2 vector for in vitro transcription of capped RNA with the mMessage mMachine Kit (Ambion). A monomeric red fluorescent protein (mRFP1) fusion with actin (generous gift of Shelly Halpain) was expressed in the same way. The RNA was then purified with Qiagen RNeasy Mini Kit and a subsequent ethanol precipitation step.

Immunohistochemistry

Immunohistochemistry and in situ hybridization procedures and embryonic dissections were performed as described by Van Vactor and Kopczynski (1999). Embryos were incubated in monoclonal 1D4 (anti-FasII) antibody (1:5) overnight at 4°C. Anti-engrailed antibody (4D9; 1:1) was obtained from the Developmental Studies Hybridoma Bank (DSHB) and developed with Ni-DAB. Anti-lacZ antibody (Cappel; rabbit polyclonal; 1:5000) was used to counterstain embryos from lacZ balancers. For Orbit, Slit, and Robo fluorescent immunostaining, embryos were collected at stage 16-17 and live dissected and fixed in 4% formaldehyde in PBS for 20 min. Anti-Robo (13C9; 1:10) and anti-Slit (C555.6D; 1:4) antibodies were obtained from the DSHB. Alexa 488 or 568 fluorophore-conjugated secondary antibodies (Molecular Probes; 1:500) were used. Fluoroscently stained embryos were mounted in Vectashield mounting media (Vector Labs).

Culture of *Drosophila* and *Xenopus* Neural Explants

Explants of late-stage *Drosophila* embryonic CNS were cultured as previously described (Wills et al., 1999a). *Xenopus* embryos were obtained from *Xenopus laevis* frogs (NASCO). They were fertilized in vitro, dejellied, and cultured at 14°C–18°C in 0.1× Marc's modified Ringer's (MMR) (see the Supplemental Materials at http://www.neuron.org/cgi/content/full/42/6/913/DC1). Four cell-stage embryos were placed in 0.1× MMR containing 5% Ficoll. A volume of 10 nl containing 0.5–2 ng RNA of GFP-CLASP and 0.25 ng mRFP1-actin or 0.05 ng GFP-CLIP RNA, respectively, was injected into each of the dorsal blastomeres. For detection of microtubules, 5 ng Rhodamine-conjugated Tubulin (Cytoskeleton Inc.) was coinjected with RNAs in PEM buffer (80 mM PIPES, pH 6.8; 1 mM EGTA; 1 mM $MgCl_2$).

Microscopy and Image Processing

For fixed tissue, images were obtained on an AxioplanII microscope (Carl Zeiss, Inc.) with a Spot-RT (Diagnostic Instruments) camera and Openlab3 software (Improvision). Laser-scanning confocal analysis was performed on a BioRad Radience instrument with a Nikon E800 platform; deconvolution was performed with either Autoquant or Velocity (Improvision) software. Phenotypic quantification was typically performed blind of genotype and from multiple experiments to ensure reproducibility. For methodological detail on imaging of *Xenopus* growth cones, refer to the Supplemental Materials at http://www.neuron.og/cgi/content/full/42/6/913/DC1.

Acknowledgments

We would like to thank Drs. Tim Mitchison and Frank Gertler for many helpful discussions and constructive criticism. We thank Kristen Kwan and Marc Kirschner for their generous assistance in learning how to manipulate *Xenopus* embryos. We are extremely grateful to Dr. Shelley Halpain for generously providing the unpublished mRFP1-actin construct. We also thank Drs. Niels Galjart, Claudio Sunkel, David Glover, and Greg Bashaw for providing published reagents. We thank Jennifer Waters Shuler and Lara Petrak at the Nikon Imaging Center at Harvard Medical School for expert advice and assistance in confocal microscopy and digital image processing. We also thank the DSHB for its repository of available antibodies; the DSHB was developed under the auspices of NICHD and maintained by the University of Iowa Department of Biological Sciences. U.E. was supported by a fellowship from the Swiss National Science Foundation. D.V.V. is a Leukemia and Lymphoma Society Scholar and is supported by grants from NINDS (NS35909 and NS40043).

Received: February 25, 2004
Revised: April 16, 2004
Accepted: May 5, 2004
Published: June 23, 2004

References

Akhmanova, A., Hoogenraad, C.C., Drabek, K., Stepanova, T., Dortland, B., Verkerk, T., Vermeulen, W., Burgering, B.M., De Zeeuw, C.I., Grosveld, F., and Galjart, N. (2001). Clasps are CLIP-115 and -170 associating proteins involved in the regional regulation of microtubule dynamics in motile fibroblasts. Cell *104*, 923–935.

Bashaw, G.J., Kidd, T., Murray, D., Pawson, T., and Goodman, C.S. (2000). Repulsive axon guidance: Abelson and Enabled play opposing roles downstream of the roundabout receptor. Cell *101*, 703–715.

Buck, K.B., and Zheng, J.Q. (2002). Growth cone turning induced by direct local modification of microtubule dynamics. J. Neurosci. *22*, 9358–9367.

Carvalho, P., Tirnauer, J.S., and Pellman, D. (2003). Surfing on microtubule ends. Trends Cell Biol. *13*, 229–237.

Cowan, C.A., and Henkemeyer, M. (2001). The SH2/SH3 adaptor Grb4 transduces B-ephrin reverse signals. Nature *413*, 174–179.

Crowner, D., Le Gall, M., Gates, M.A., and Giniger, E. (2003). Notch steers *Drosophila* ISNb motor axons by regulating the Abl signaling pathway. Curr. Biol. *13*, 967–972.

Dehmelt, L., and Halpain, S. (2004). Actin and microtubules in neurite initiation: are MAPs the missing link? J. Neurobiol. *58*, 18–33.

Dent, E.W., and Gertler, F.B. (2003). Cytoskeletal dynamics and transport in growth cone motility and axon guidance. Neuron *40*, 209–227.

Dent, E.W., and Kalil, K. (2001). Axon branching requires interactions between dynamic microtubules and actin filaments. J. Neurosci. *21*, 9757–9769.

Dickson, B.J. (2002). Molecular mechanisms of axon guidance. Science *298*, 1959–1964.

Elkins, T., Zinn, K., McAllister, L., Hoffmann, F.M., and Goodman, C.S. (1990). Genetic analysis of a *Drosophila* neural cell adhesion molecule: interaction of fasciclin I and Abelson tyrosine kinase mutations. Cell *60*, 565–575.

Etienne-Manneville, S., and Hall, A. (2002). Rho GTPases in cell biology. Nature *420*, 629–635.

Fan, J., and Raper, J.A. (1995). Localized collapsing cues can steer growth cones without inducing their full collapse. Neuron *14*, 263–274.

Fan, J., Mansfield, S.G., Redmond, T., Gordon-Weeks, P.R., and Raper, J.A. (1993). The organization of F-actin and microtubules in growth cones exposed to a brain-derived collapsing factor. J. Cell Biol. *121*, 867–878.

Fan, X., Labrador, J.P., Hing, H., and Bashaw, G.J. (2003). Slit stimulation recruits Dock and Pak to the roundabout receptor and increases Rac activity to regulate axon repulsion at the CNS midline. Neuron *40*, 113–127.

Fedorova, S.A., Chubykin, V.L., Gusachenko, A.M., and Omel'yanchuk, L.V. (1997). Mutation chromosome bows (chbv40), associated with the abnormal chromosome spindle in Drosophila melanogaster. Russ. J. Genet. *33*, 1286–1292.

Fukata, M., Watanabe, T., Noritake, J., Nakagawa, M., Yamaga, M., Kuroda, S., Matsuura, Y., Iwamatsu, A., Perez, F., and Kaibuchi, K. (2002a). Rac1 and Cdc42 capture microtubules through IQGAP1 and CLIP-170. Cell *109*, 873–885.

Fukata, Y., Itoh, T.J., Kimura, T., Menager, C., Nishimura, T., Shiromizu, T., Watanabe, H., Inagaki, N., Iwamatsu, A., Hotani, H., and Kaibuchi, K. (2002b). CRMP-2 binds to tubulin heterodimers to promote microtubule assembly. Nat. Cell Biol. *4*, 583–591.

Gertler, F.B., Comer, A.R., Juang, J.-L., Ahern, S.M., Clark, M.J., Liebl, E.C., and Hoffmann, F.M. (1995). enabled, a dosage-sensitive suppressor of mutations in the Drosophila Abl tyrosine kinase, encodes an Abl substrate with SH3 domain-binding properties. Genes Dev. *9*, 521–533.

Giniger, E. (1998). A role for Abl in Notch signaling. Neuron *20*, 667–681.

Goold, R.G., and Gordon-Weeks, P.R. (2001). Microtubule-associated protein 1B phosphorylation by glycogen synthase kinase 3beta is induced during PC12 cell differentiation. J. Cell Sci. *114*, 4273–4278.

Gordon-Weeks, P.R. (2004). Microtubules and growth cone function. J. Neurobiol. *58*, 70–83.

Goshima, Y., Nakamura, F., Strittmatter, P., and Strittmatter, S.M. (1995). Collapsin-induced growth cone collapse mediated by an intracellular protein related to UNC-33. Nature *376*, 509–514.

Grevengoed, E.E., Loureiro, J.J., Jesse, T.L., and Peifer, M. (2001). Abelson kinase regulates epithelial morphogenesis in Drosophila. J. Cell Biol. *155*, 1185–1198.

Hely, T.A., and Willshaw, D.J. (1998). Short-term interactions between microtubules and actin filaments underlie long-term behavior in neuronal growth cones. Proc. R. Soc. Lond. B. Biol. Sci. *265*, 1801–1807.

Henkemeyer, M.J., Gertler, F.B., Goodman, W., and Hoffmann, F.M. (1987). The *Drosophila* Abelson proto-oncogene homolog: identification of mutant alleles that have pleiotropic effects late in development. Cell *51*, 821–828.

Hsouna, A., Kim, Y.S., and VanBerkum, M.F. (2003). Abelson tyrosine kinase is required to transduce midline repulsive cues. J. Neurobiol. *57*, 15–30.

Hummel, T., Krukkert, K., Roos, J., Davis, G., and Klambt, C. (2000). *Drosophila* Futsch/22C10 is a MAP1B-like protein required for dendritic and axonal development. Neuron *26*, 357–370.

Inoue, Y.H., do Carmo Avides, M., Shiraki, M., Deak, P., Yamaguchi, M., Nishimoto, Y., Matsukage, A., and Glover, D.M. (2000). Orbit, a novel microtubule-associated protein essential for mitosis in Drosophila melanogaster. J. Cell Biol. *149*, 153–166.

Jordan, J.D., Landau, E.M., and Ivenger, R. (2000). Signaling networks: the origins of cellular multitasking. Cell *103*, 193–200.

Kalil, K., Szebenyi, G., and Dent, E.W. (2000). Common mechanisms underlying growth cone guidance and axon branching. J. Neurobiol. *44*, 145–155.

Kidd, T., Bland, K.S., and Goodman, C.S. (1999). Slit is the midline repellent for the robo receptor in *Drosophila*. Cell *96*, 785–794.

Komarova, Y.A., Akhmanova, A.S., Kojima, S., Galjart, N., and Borisy, G.G. (2002). Cytoplasmic linker proteins promote microtubule rescue in vivo. J. Cell Biol. *159*, 589–599.

Lanier, L.M., and Gertler, F.B. (2000). From Abl to actin: Abl tyrosine kinase and associated proteins in growth cone motility. Curr. Opin. Neurobiol. *10*, 80–87.

Lanier, L.M., Gates, M.A., Witke, W., Menzies, A.S., Wehman, A.M., Macklis, J.D., Kwiatkowski, D., Soriano, P., and Gertler, F.B. (1999). Mena is required for neurulation and commissure formation. Neuron *22*, 313–325.

Lebrand, C., Dent, E.W., Strasser, G.A., LoLanier, L.M., Krause, M., Svitkina, T.M., Borisy, G.G., and Gertler, F.B. (2004). Critical role of Ena/VASP proteins for filopodia formation in neurons and in function downstream of Netrin-1. Neuron, in press.

Lee, S., and Kolodziej, P.A. (2002). Short Stop provides an essential link between F-actin and microtubules during axon extension. Development *129*, 1195–1204.

Lee, H., and Van Vactor, D. (2003). Neurons take shape. Curr. Biol. *13*, R152–R161.

Lee, S., Harris, K.L., Whitington, P.M., and Kolodziej, P.A. (2000). short stop is allelic to kakapo, and encodes rod-like cytoskeletal-associated proteins required for axon extension. J. Neurosci. *20*, 1096–1108.

Lemos, C.L., Sampaio, P., Maiato, H., Costa, M., Omel'yanchuk, L.V., Liberal, V., and Sunkel, C.E. (2000). Mast, a conserved microtubule-associated protein required for bipolar mitotic spindle organization. EMBO J. *19*, 3668–3682.

Liebl, E.C., Forsthoefel, D.J., Franco, L.S., Sample, S.H., Hess, J.E., Cowger, J.A., Chandler, M.P., Shupert, A.M., and Seeger, M.A. (2000). Dosage-sensitive, reciprocal genetic interactions between the Abl tyrosine kinase and the putative GEF Trio reveal Trio's role in axon pathfinding. Neuron *26*, 107–118.

Liebl, E.C., Rowe, R.G., Forsthoefel, D.J., Stammler, A.L., Schmidt, E.R., Turski, M., and Seeger, M.A. (2003). Interactions between the secreted protein Amalgam, its transmembrane receptor Neurotactin and the Abelson tyrosine kinase affect axon pathfinding. Development *130*, 3217–3226.

Lin, C., and Forscher, P. (1993). Cytoskeletal remodeling during growth cone-target interactions. J. Cell Biol. *121*, 1369–1383.

Loureiro, J., and Peifer, M. (1998). Roles of Armadillo, a *Drosophila* catenin, during central nervous system development. Curr. Biol. *8*, 622–632.

Loureiro, J.J., Rubinson, D.A., Bear, J.E., Baltus, G.A., Kwiatkowski, A.V., and Gertler, F.B. (2002). Critical roles of phosphorylation and actin binding motifs, but not the central proline-rich region, for Ena/vasodilator-stimulated phosphoprotein (VASP) function during cell migration. Mol. Biol. Cell *13*, 2533–2546.

Lundgren, S.E., Callahan, C.A., Thor, S., and Thomas, J.B. (1995). Control of neuronal pathway selection by the Drosophila LIM homeodomain gene apterous. Development *121*, 1769–1773.

Luo, L., Liao, Y.J., Jan, L.Y., and Jan, Y.N. (1994). Distinct morphogenetic functions of similar small GTPases: Drosophila Drac1 is involved in axonal outgrowth and myoblast fusion. Genes Dev. *8*, 1787–1802.

Maiato, H., Sampaio, P., Lemos, C.L., Findlay, J., Carmena, M., Earnshaw, W.C., and Sunkel, C.E. (2002). MAST/Orbit has a role in microtubule-kinetochore attachment and is essential for chromosome alignment and maintenance of spindle bipolarity. J. Cell Biol. *157*, 749–760.

Maiato, H., Rieder, C.L., Earnshaw, W.C., and Sunkel, C.E. (2003). How do kinetochores CLASP dynamic microtubules? Cell Cycle *2*, 511–514.

Miller, A.L., Wang, Y., Mooseker, M.S., and Koleske, A.J. (2004). The Abl-related gene (Arg) requires its F-actin-microtubule cross-linking activity to regulate lamellipodial dynamics during fibroblast adhesion. J. Cell Biol. *165*, 407–419.

Moresco, E.M., and Koleske, A.J. (2003). Regulation of neuronal morphogenesis and synaptic function by Abl family kinases. Curr. Opin. Neurobiol. *13*, 535–544.

Murray, M.J., Merritt, D.J., Brand, A.H., and Whitington, P.M. (1998). In vivo dynamics of axon pathfinding in the Drosophila CNS: a time-lapse study of an identified motorneuron. J. Neurobiol. *37*, 607–621.

Myers, P.Z., and Bastiani, M.J. (1993). Growth cone dynamics during the migration of an identified commissural growth cone. J. Neurosci. *13*, 127–143.

Nishimura, T., Fukata, Y., Kato, K., Yamaguchi, T., Matsuura, Y., Kamiguchi, H., and Kaibuchi, K. (2003). CRMP-2 regulates polarized Numb-mediated endocytosis for axon growth. Nat. Cell Biol. *5*, 819–826.

O'Connor, T.P., and Bentley, D. (1993). Accumulation of actin in subsets of pioneer growth cone filopodia in response to neural and epithelial guidance cues in situ. J. Cell Biol. *123*, 935–948.

Patel, B., and Van Vactor, D. (2002). Axon guidance: the cytoplasmic tail. Current Opin. Cell Biol. *14*, 221–229.

Rajagopalan, S., Vivancos, V., Nicolas, E., and Dickson, B.J. (2000). Selecting a longitudinal pathway: Robo receptors specify the lateral position of axons in the *Drosophila* CNS. Cell *103*, 1033–1045.

Rhee, J., Mahfooz, N.S., Arregui, C., Lilien, J., Balsamo, J., and VanBerkum, M.F. (2002). Activation of the repulsive receptor Roundabout inhibits N-cadherin-mediated cell adhesion. Nat. Cell Biol. *4*, 798–805.

Rodriguez, O.C., Schaefer, A.W., Mandato, C.A., Forscher, P., Bement, W.M., and Waterman-Storer, C.M. (2003). Conserved microtubule-actin interactions in cell movement and morphogenesis. Nat. Cell Biol. *5*, 599–609.

Rothenberg, M.E., Rogers, S.L., Vale, R.D., Jan, L.Y., and Jan, Y.N. (2003). *Drosophila* pod-1 crosslinks both actin and microtubules and controls the targeting of axons. Neuron *39*, 779–791.

Rusch, J., and Van Vactor, D. (2000). New Roundabouts send axons into the Fas lane. Neuron *28*, 637–640.

Sabry, J.H., O'Connor, T.P., Evans, L., Toroian-Raymond, A., Kirschner, M., and Bentley, D. (1991). Microtubule behavior during guidance of pioneer neuron growth cones in situ. J. Cell Biol. *115*, 381–395.

Schaefer, A.W., Kabir, N., and Forscher, P. (2002). Filopodia and actin arcs guide the assembly and transport of two populations of microtubules with unique dynamic parameters in neuronal growth cones. J. Cell Biol. *158*, 139–152.

Schwab, M.E. (2000). Finding the lost target. Nature *403*, 259–260.

Seeger, M., Tear, G., Ferres-Marco, D., and Goodman, C.S. (1993). Mutations affecting growth cone guidance in *Drosophila*: genes necessary for guidance toward or away from the midline. Neuron *3*, 409–426.

Shamah, S.M., Lin, M.Z., Goldberg, J.L., Estrach, S., Sahin, M., Hu, L., Bazalakova, M., Neve, R.L., Corfas, G., Debant, A., and Greenberg, M.E. (2001). EphA receptors regulate growth cone dynamics through the novel guanine nucleotide exchange factor ephexin. Cell *105*, 233–244.

Stepanova, T., Slemmer, J., Hoogenraad, C.C., Lansbergen, G., Dortland, B., De Zeeuw, C.I., Grosveld, F., van Cappellen, G., Akhmanova, A., and Galjart, N. (2003). Visualization of microtubule growth in cultured neurons via the use of EB3-GFP (end-binding protein 3-green fluorescent protein). J. Neurosci. *23*, 2655–2664.

Subramanian, A., Prokop, A., Yamamoto, M., Sugimura, K., Uemura, T., Betschinger, J., Knoblich, J.A., and Volk, T. (2003). Shortstop recruits EB1/APC1 and promotes microtubule assembly at the muscle-tendon junction. Curr. Biol. *13*, 1086–1095.

Suter, D.M., and Forscher, P. (1998). An emerging link between cytoskeletal dynamics and cell adhesion molecules in growth cone guidance. Curr. Opin. Neurobiol. *8*, 106–116.

Suter, D.M., and Forscher, P. (2000). Substrate-cytoskeletal coupling as a mechanism for the regulation of growth cone motility and guidance. J. Neurobiol. *44*, 97–113.

Tanaka, E.M., and Kirschner, M.W. (1991). Microtubule behavior in the growth cones of living neurons during axon elongation. J. Cell Biol. *115*, 345–363.

Tanaka, E.M., Ho, T., and Kirschner, M.W. (1995). The role of microtubule dynamics in growth cone motility and axonal growth. J. Cell Biol. *128*, 139–155.

Thomas, J.B., Bastiani, M.J., Bate, M., and Goodman, C.S. (1984). From grasshopper to Drosophila: a common plan for neuronal development. Nature *310*, 203–207.

Van Vactor, D., and Kopczynski, C. (1999). Techniques for anatomical analysis of the Drosophila embryonic nervous system. In A Comparative Methods Approach to the Study of Oocytes and Embryos, J. Richter, ed. (New York: Oxford University Press), pp. 490–513.

Van Vactor, D., Sink, H., Fambrough, D., Tsoo, R., and Goodman, C.S. (1993). Genes that control neuromuscular specificity in *Drosophila*. Cell *73*, 1137–1153.

Williamson, T., Gordon-Weeks, P.R., Schachner, M., and Taylor, J. (1996). Microtubule reorganization is obligatory for growth cone turning. Proc. Natl. Acad. Sci. USA *93*, 15221–15226.

Wills, Z., Marr, L., Zinn, K., Goodman, C.S., and Van Vactor, D. (1999a). Profilin and the Abl tyrosine kinase are required for motor axon outgrowth in the *Drosophila* embryo. Neuron *22*, 291–299.

Wills, Z., Bateman, J., Korey, C., Comer, A., and Van Vactor, D. (1999b). The tyrosine kinase Abl and its substrate Enabled collaborate with the receptor phosphatase Dlar to control motor axon guidance. Neuron *22*, 301–312.

Wills, Z., Emerson, M., Rusch, J., Bikoff, J., Baum, B., Perrimon, N., and Van Vactor, D. (2002). A *Drosophila* homolog of cyclase-associated proteins collaborates with the Abl tyrosine kinase to control midline axon pathfinding. Neuron *36*, 611–622.

Wittmann, T., Bokoch, G.M., and Waterman-Storer, C.M. (2003). Regulation of leading edge microtubule and actin dynamics downstream of Rac1. J. Cell Biol. *161*, 845–851.

Zhou, F.Q., Waterman-Storer, C.M., and Cohan, C.S. (2002). Focal loss of actin bundles causes microtubule redistribution and growth cone turning. J. Cell Biol. *157*, 839–849.